Optimized electrode formulation for enhanced performance of graphite in K-ion batteries

Badre Larhrib, Lénaïc Madec, Laure Monconduit, Hervé Martinez

Optimized electrode formulation for enhanced performance of graphite in K-ion batteries.

Badre Larhrib[a], Lénaïc Madec[a,c,*], Laure Monconduit[b,c], Hervé Martinez[a,c]

[a] Universite de Pau et des Pays de l'Adour, E2S UPPA, CNRS, IPREM, Pau, France

[b] ICGM, Université de Montpellier, CNRS, Montpellier (France)

[c] Réseau sur le Stockage Electrochimique de l'Energie, CNRS FR3459, Amiens, France

* Corresponding author: lenaic.madec@univ-pau.fr

ABSTRACT

Potassium ion batteries (KIBs) are emerging notably due to the reversible K^+ intercalation into graphite. So far, optimization of graphite electrode formulation remains, however, to be investigated. This work thus proposes to optimize ionic (porosity) and electronic percolation networks as well as mechanical properties of graphite electrodes for KIBs. To do so, carbon black amount (CB) and electrode calendering is first adjusted. Then carboxylated styrene butadiene rubber (SBR) is used, with different amount and functional groups contents, as co-binder with carboxymethyl cellulose (CMC-Na). The best electrodes, made of 95/5/8/2 wt.% of graphite(SLP30)/CB(C65)/CMC-Na/SBR(Synthomer) with 2.4 mg cm^{-2} loading and 35% porosity, deliver ~250 mAh g^{-1} during depotassiation at 5C with only ~0.3 V polarization and 205 mAh g^{-1} during potassiation at 1C (3-electrodes configuration). In addition, no capacity loss is observed after 55 cycles at C/5 potassiation/1C depotassiation due to a low electrode volume expansion (11%) compared to 24% without SBR after only 35 cycles. These results highlight that appropriate SBR significantly improves the electrode structure/cohesion/elasticity (i.e. volume expansion management), leading to better power performance and capacity retention of graphite electrodes for KIBs. Finally, considering that further improvements are expected by tuning electrolyte formulation, this work will benefit to the development of high energy KIBs.

1. INTRODUCTION

Potassium-ion batteries (KIBs) are considered as an attractive technology due to the K abundance (2.1 wt.% of the Earth's crust) [1] and low standard redox potential of K^+/K (−2.93 V vs. SHE), which is close to that of Li^+/Li (−3.04 V vs. SHE). In addition, K^+ presents the smallest Stokes' radius (3.6 Å) in propylene carbonate compared to Li^+ (4.8 Å) and Na^+ (4.6 Å) so that electrolytes with higher ionic conductivity are expected in KIBs (i.e. high power cells) [2]. More importantly, similarly to Li^+ and contrary to Na^+, the electrochemical intercalation of K^+ into graphite interlayers was experimentally demonstrated by Komaba et al. [3], thus allowing its use as active material for negative electrode in KIBs. However, compared with the size of Li^+ (0.76 Å), the oversize of K^+ (1.38 Å) leads to a much higher volume expansion (60% compared to 13% with Li^+) so that during the potassiation/depotassiation processes, both graphite structure damages and electrode pulverization/delamination may occur [4]. In the latter case, it is thus of great interest to evaluate and control the volume expansion of the electrode upon cycling.

Regarding the formation of the so-called K-graphite intercalation compounds (K-GICs), studies based on both theoretical and experimental approaches have proposed different mechanisms. Based on ex situ X-ray diffraction (XRD), the following mechanism was proposed: C → KC_{36} (stage III at 0.3–0.2 V) → KC_{24} (stage II at 0.2-0.15 V) → KC_8 (stage I at 0.15-0.01 V). Then, depotassiation KC_8 leads back to graphite while in following cycles, XRD showed structural damage of the graphite explained by the high-volume expansion (60%) [5]. Based on density-functional theory (DFT) calculations and ex situ XRD and Raman, a slightly different mechanism was proposed: C → KC_{24} (stage III, between 0.35 and 0.18 V) → KC_{16} (stage II at 0.14 V) → KC_8 (stage I at 0.01 V) [22]. Based on in situ XRD and Raman as well as DFT, a mechanism starting from dilute stage was proposed: KC_{60} (stage V) → KC_{48} (stage IV) → KC_{36} (stage III) → KC_{24}/KC_{16} (stage II) → KC_8 (stage I) [6]. Overall, full potassiation of graphite leads to KC_8 (60% volume expansion) corresponding to a 279 mAh g^{-1} theoretical capacity. However, conventional graphite delivers about 65% of its capacity between 0.25 V and 0.01 V so that power performance could be limited if the K^+ mobility is low during graphite potassiation, which still need to be confirmed. So far, power performance of graphite in half-cells are significantly altered by the large K metal plating/stripping polarization [7,32]. For instance, this polarization is about 0.1 V higher with 0.8M KFSI EC:DEC compared to 0.8M KPF_6 EC:DEC, which explains the lower rate performance generally observed with KFSI [8,9].

It is thus of high interest to better evaluate and control the parameters that govern the energy and power performance of graphite-based electrodes in KIBs. So far, most of the studies focused on the electrolyte formulation (solvents and salt(s) ratios) to form a stable/passivating solid electrolyte interphase (SEI) without hindering the power performance [10-15]. However, half-cells results should be taken with caution as the highly reactive K metal was proved to significantly affect electrochemical performance (K metal polarization) [3,7,8,32] as well as the SEI formation (cross talking mechanism) [16,17,33]. Considering the electrode materials and formulation, i.e. the graphite structure, the conductive additives, binders, active material loading and calendering pressure, only a limited number of studies have been performed. Indeed, studies about carbon additives and calendering pressure effects are still missing in the literature while they are expected to critically impact both ionic and electronic percolation networks (power performance), similarly to Li-ion batteries (LIBs) [18]. In particular, the use of carbon black with nanoscale primary particles size (compared to microscale for graphite) is mandatory to form an efficient/durable percolating electronic network. Calendering will also affect the cohesion and adhesion between graphite particles and binder(s) as well as with the current collector, which are critical parameters regarding the graphite volume expansion issue [19]. Regarding the graphite structure (interlayer distance and defects), polynanocrystalline graphite, made by chemical vapor deposition on a nanoporous graphenic carbon matrix, was used to increase the capacity retention thanks to the presence of disorder at nanoscales but strict order at atomic scales [20]. Expanded graphite with enlarged interlayer spaces have also been proposed to boost the potassium ion diffusion with a capacity up to ~175 mAh g^{-1} at 200 mA g^{-1} rate (for 2 $mg_{graphite}$ cm^{-2} electrode) compared to ~40 mAh g^{-1} for a conventional graphite [21]. Ball milling during electrode slurry preparation was also reported to increase capacity retention due to gentle graphene layers exfoliation and defects formation [22]. The aim of these graphite structure modification is to mitigate graphite structural damages induced by the volume expansion. A study showed, however, that graphite electrodes (with, however, unknown graphite supplier, type and loading) can cycle more than 2000 times as C/3 with nearly no capacity loss while the same graphite electrodes with a 28.56 mg cm^{-2} loading also showed no capacity loss after 60 cycles at C/14 [13]. Despite missing information about the graphite electrodes, these results suggest that both structural damages and/or electrode pulverization induced by the volume expansion may not be an issue. Regarding the binders (amount and type), their roles are to obtain good mechanical properties (especially for the electrode processing) as well as to maintain the electrode cohesion / limit the electrode volume expansion upon cycling. So far, polyvinylidene fluoride (PVDF), sodium polyacrylate

(sodium polyacrylic acid, PAA-Na) and sodium carboxymethylcellulose (CMC-Na) have been tested in graphite electrode for KIBs. Among them, PAA-Na and CMC-Na showed significant increase of the coulombic efficiency (CE) to due to a pre-formed SEI induced by the binders while PAA-Na led to higher capacity retention due its lower swelling property [3,23]. Another study also pointed out that generally, binder amount higher than 4 wt.% (literature data), for instance 8 wt.% (their data with a 1:1 weight ratio of CMC-Na/PAA), significantly increases the capacity retention of graphite electrodes for KIBs [24].

However, styrene-butadiene rubber (SBR, especially carboxylated ones), frequently used as high elasticity binder with good mechanical properties for graphite electrodes in LIBs [5,25,26,34], has never been tested in KIBs so far. Additionally, the combination of SBR with CMC is known to produce more homogeneous and less microporous graphite electrodes [27] due to an increase of the graphite surface charge, as established by electrokinetic measurements [28]. In addition, both SBR and CMC are water-soluble binders with low cost and pollution as well as fast-drying kinetics in electrode fabrication [29]. Overall, the literature thus highlights that electrode formulation (conductive additive and binder(s) amounts as well as graphite loading and calendering pressure…) is the key towards high performance graphite electrodes for KIBs. However, the concomitant study of these electrode formulation parameters is still missing so far, and especially for KIBs.

To fill this gap, this work evaluates the effects of the carbon black amount together with the electrode calendering on the electrochemical performance of graphite electrodes with two different loadings for KIBs. Subsequently, the impact of SBR with different amount and functional groups contents as co-binder with CMC-Na are also investigated. At each step, a focus is performed on the CE, capacity retention and more importantly on polarization / rate capability. Overall, the aim of this study is to get high-capacity Gr//K cells with enhanced cycling performance in order to develop high energy KIBs in the future.

2. EXPERIMENTAL

Materials and electrodes preparation

Graphite SLP30 (Gr, from TIMCAL), carbon black Super C65 (CB, from MTI) and CMC-Na (noted CMC thereafter, Sigma-Aldrich, Mw ~250000) were used as active material, conductive additive, and binder, respectively. Two carboxylated SBR binders (noted SBR,

kindly provided by nanografi and SBR(2), kindly provided by Synthomer) were also used as co-binders with CMC (see Table S1 for their physical and chemical properties). Electrode slurries were prepared by mixing different amounts of materials (**Figure 1**) in distilled water using mechanical planetary ball milling (PULVERISETTE 7) at 500 rpm for 1h. Slurries were coated on an aluminum current collector foil with a 15 nm thickness using the doctor blade method with a blade thickness of 125 or 200 µm for the 2.4 mg cm^{-2} and 4 mg cm^{-2} graphite loading, respectively. Films were then dried at room temperature for 1 night. Electrodes were then cut out with a 12.7 mm diameter using a precision punch and dried again in a vacuum oven at 80 °C for 12 h.

The strategy to optimize the Gr electrodes formulation is presented in **Figure 1**. In the first step, the CMC amount was kept constant (10 wt.%) while the Gr/CB amounts (in wt.%) were varied as follow: 88/2, 85/5 and 82/8. For each composition, two loadings (2.4 and 4 $mg_{graphite}$ cm^{-2}) were prepared with different uniaxial calendering loads (1, 2, 3, 4 and 5 tons, i.e. 1.05, 2.10, 3.18, 4.21 and 5.26 tons cm^{-2}, respectively) in order to obtain optimal ionic(porosity)/electronic percolation networks. In the second step, the effect of CMC/SBR as co-binders on the electrode structure and mechanical properties was evaluated (**Figure 1**). To do so, the optimal Gr/CB contents, graphite loading, and calendering pressure were selected and only the CMC/SBR contents were varied as follow: 10/0, 8/2, 6/4 (in wt.%). In a third step, another SBR (Synthomer one) was used with the previously optimized CMC/SBR contents in order to evaluate the impact of the SBR nature (i.e. functional groups contents and despite that such information is not available for this SBR, **Table S1**) on the electrochemical performance. Finally, to evaluate the impact of two SBR on the electrode volume expansion, electrodes thickness was measured before and after cycling using a micrometer (Mitutoyo with an accuracy of ±1 µm).

Electrochemical experiments

Electrochemical tests were performed by assembling CR2032 coin half-cells as follow: graphite (Gr) electrodes, microporous trilayer (PP/PE/PP, from Celgard) and glass fiber (GF/D, from Whatman) membranes as separator, K metal (Alfa Aesar, 99.95%) as reference with 0.8 M KPF_6 (Sigma-Aldrich, ≥99%) EC:DEC (ethylene carbonate, Sigma-Aldrich, ≥99% and diethyl carbonate, Sigma-Aldrich, ≥99%) 1:1 by volume as electrolyte. All tests were conducted on two pair cells (for reproducibility) using a VMP 3 multichannel system (BioLogic, France) in a 20°C temperature-controlled room.

Rate performance was evaluated using a standard galvanostatic cycling procedure as follow: between 2-0.01V, 3 formation cycles (or 5 for the CMC/SBR study) at C/20, 5 cycles at C/10, C/5, C/2, C, 2C, 5C, 10C followed by 5 cycles at C/10 and C/20 to check for possible capacity loss. Importantly, for cycles performed between C/2 to 10C, potassiation was kept at C/5 to mitigate the impact of the K metal polarization (**Figure S1**). In addition, an alternative test was used to evaluate only the depotassiation rate capability as follow: between 2-0.01 V, 4 formation cycles at C/20, potassiation at C/20 followed by successive depotassiation (at xC from x= 5, 1, 0.5, 0.2, 0.1, 0.05, i.e. from 5C to C/20) and 30 min relaxation steps.

A similar procedure was used to evaluate the potassiation rate capability, using 3-electrodes Swagelok T-cells as follow: between 2-0.01 V, 4 formation cycles at C/20, followed by successive potassiation (at xC from x= 5, 2, 1, 0.2, 0.1, 0.05, i.e. from 5C to C/20) and 30 min relaxation steps. In this experiment, the cells were in PFA material, K metal was used as reference and counter electrodes, the electrolyte was 0.8 M KPF_6 EC:DEC and GF/D membrane was used as separator in contact with K metal while and additional PP/PE/PP membrane was added in contact with the graphite electrode.

Capacity retention was evaluated as follow: between 2-0.01 V, 3 formation cycles (or 5 for the CMC/SBR study) at C/20 followed by about 50 cycles at C/5 during potassiation and C during depotassiation.

Galvanostatic intermittent titration technique (GITT) was also used to discriminate the graphite polarization from the K metal one in the case of the CMC/SBR study as follow: during the first potassiation down to 0.01 V, successive 30 min constant current (-20 mA/g, i.e. 0.025 K^+ intercalation) and 8h relaxation steps were applied.

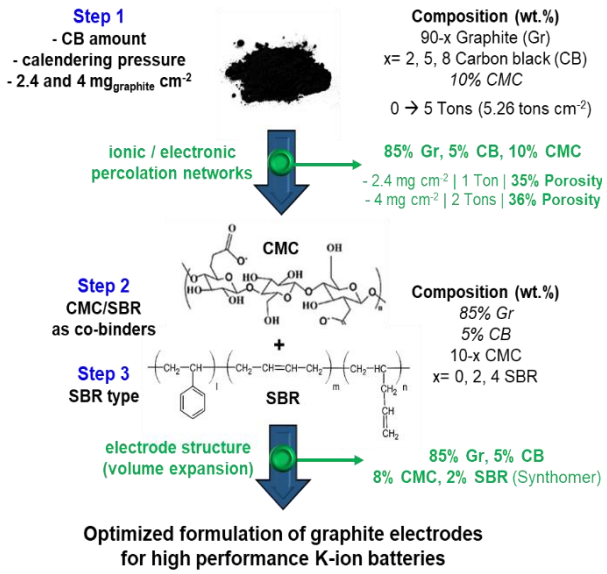

Figure 1. Schematic representation of the approach followed in this work to optimize the graphite electrodes for KIBs. For each step, the goal and optimized results obtained in this study are highlighted in green.

3. RESULTS AND DISCUSSION

3.1 Impact of carbon black amount and electrode calendering

The aim of this part is to find optimal conductive carbon black (CB) amount and calendering pressure, i.e. to reach the best balance between electronic and ionic properties of graphite electrode in KIBs. The impact of the electrode loading was also evaluated. **Figure 2** shows galvanostatic profiles during the 1st cycle at C/20 for 4 mg cm^{-2} Gr electrodes densified at 0, 1, 2, and 5 tons as function of the Gr/CB amounts. For clarity, **Figure S2** shows the obtained porosity and pores volume for the different electrode formulations while **Table S2** gathers the first cycle reversible capacity and coulombic efficiency (CE). Increasing the calendering pressure up to 1 or 2 tons enhances the delivered capacity whatever the Gr/CB amounts are. This is more likely due to an improvement of the electronic contacts between Gr particles and the CB network (*i.e.* contacts quality and numbers). However, very low capacities were obtained at 5 tons and despite the C/20 rate, which is explained by the concomitant low porosities (<20%, **Figure S2**), i.e. high ionic limitations. In addition, as the pressure increased, the delivered capacity of the electrode containing 8 wt.% of CB decreased compared to electrodes with lower CB amounts. For such high carbon content, the CMC amount (10 wt.%) is probably not enough to completely coat both the graphite and carbon

particles, leading to electrodes with poor mechanical properties. Thus, when the calendering pressure increased, the high volume expansion induced by the graphite potassiation more likely lead to partial pulverization/disconnection of the electrode while lower calendering pressure (i.e. higher electrode porosity) may help to buffer the volume expansion. Regarding the CE, improvements were obtained as the pressure (except for 5 tons) and CB amount increased. Overall, the favorable CB amount in term of both capacity and CE is 5 wt.%. The optimal calendering pressure is between 1 and 2 tons, which corresponds to electrode porosity between 43 and 36%, respectively.

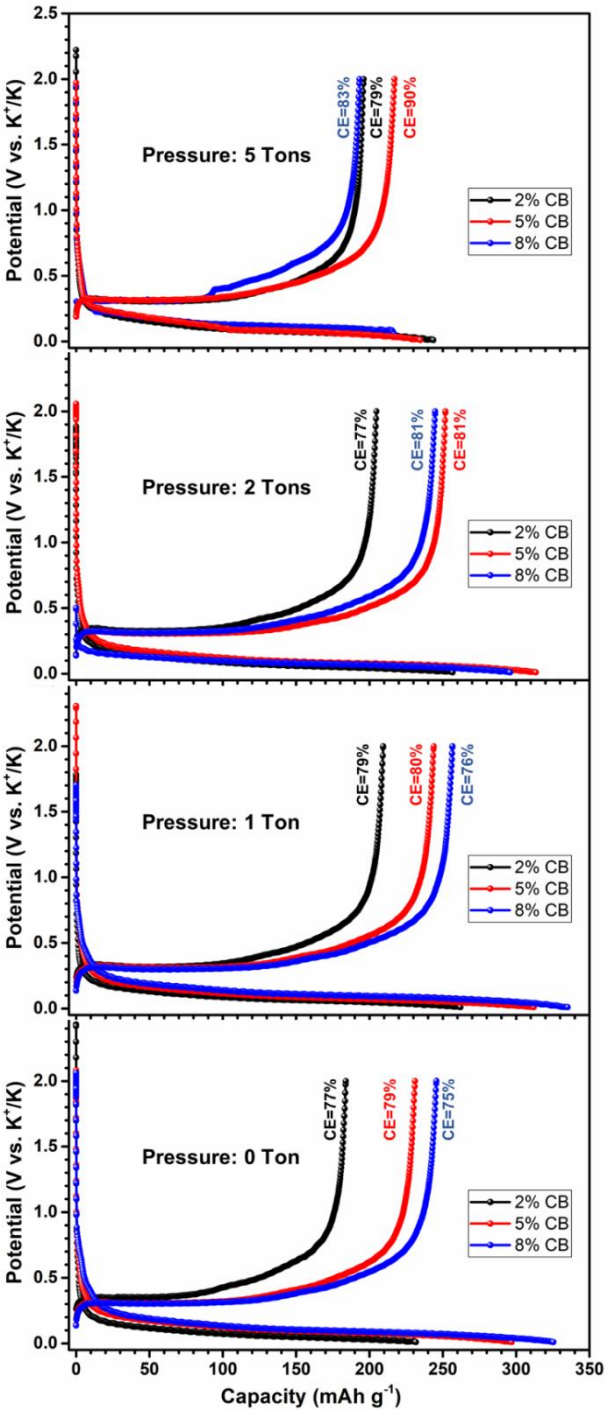

Figure 2. 1st cycle galvanostatic discharge/charge profiles between 2-0.01V at C/20 for graphite electrodes (4 mg cm^{-2}), densified at 0, 1, 2 and 5 tons, as function of the Gr/CB amounts.

To discriminate further the impact of the 1 and 2 tons calendering pressures as function of the Gr/CB amounts, rate performance was then evaluated (**Figure 3**). For information, without and with 5 tons densification, very poor performance was observed due to bad electronic and

ionic percolations, respectively (**Figure S3**). However, with 5 wt.% of CB and a calendering pressure of 2 tons, significant rate performance improvement was observed due to optimal electronic and ionic percolating networks. Also note that with this electrode formulation, nearly no capacity loss (<5%) was induced by the rate test, which means that the graphitic structure remains more likely undamaged. Capacity fading as the cycles number increased is more likely due to passivation of the K metal, associated to an increase of the K metal polarization and despite the use of C/5 potassiation (for C/5 to 10C depotassiation) to limit it (**Figure S1**). Thus graphite capacities decreased as the cycling rate increased. Based on these results, both this carbon content (5 wt.%) and calendering pressure (2 tons corresponding to a 36% electrode porosity, **Figure S2**) were selected for the rest of the study.

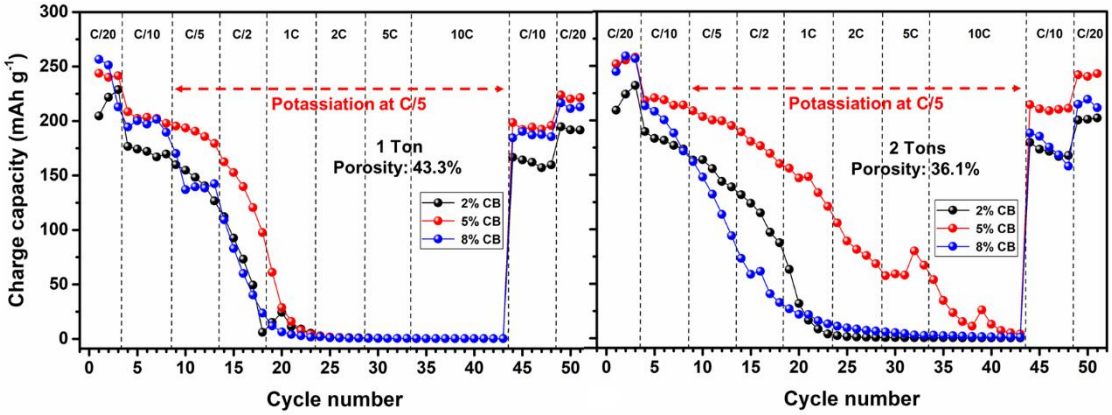

Figure 3. Rate performance obtained between 2-0.01 V for graphite electrodes (4 mg cm^{-2}), densified at 1 and 2 tons, as function of the Gr/CB amounts.

Capacity retention was then evaluated for the 4 mg cm^{-2} Gr electrodes (5wt.% CB, 36% porosity and 40 µm thickness) and compared to 2.4 mg cm^{-2} Gr electrodes (5wt.% CB, 35% porosity and 29 µm thickness), **Figure 4**. As expected, lowering the graphite loading led to a better capacity retention after 41 cycles with 210 mAh g^{-1} (only 5% loss) compared to 188 mAh g^{-1} (28% loss) for the higher loading. Note that when the 2.4 mg cm^{-2} electrodes were densified at 2 tons (corresponding to 29% porosity), a rapid capacity fading was observed (**Figure S4**), demonstrating that lowering the porosity leads to ionic limitations. At the opposite, the 4 mg cm^{-2} electrodes densified at 1 ton (43% porosity) showed higher capacity fading (**Figure S4**) but due to electronic limitations, probably increased by the volume expansion issue upon cycling. Overall, for both loadings, the optimal electrode porosity is about 35%. For the rest of the study, the 2.4 mg cm^{-2} graphite loading was selected.

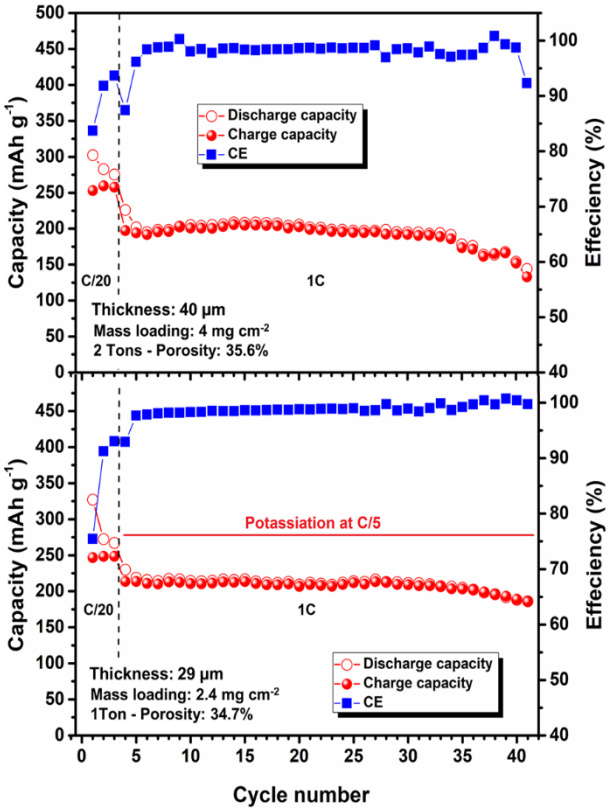

Figure 4. Capacity retention and coulombic efficiency obtained between 2-0.01 V at C/5 potassiation and 1C depotassiation rates after 3 formations cycles at C/20 for 4 and 2.4 mg cm^{-2} graphite electrodes (5wt.% CB and ~35% porosity).

3.2 Impact of SBR as co-binder

The aim of this part is to evaluate the effect of carboxylated SBR as co-binder with CMC regarding the volume expansion issue of graphite electrodes, i.e. the impact on high depotassiation rates and capacity retention. **Figure 5** shows galvanostatic profiles during the 1^{st} and 5^{th} cycles at C/20 for graphite electrodes (2.4 mg cm^{-2}, 5 wt.% CB and 35% porosity) as function of SBR/CMC amounts (0/10, 2/8 and 4/6 in wt.%). Compared with CMC only, using 2 wt.% SBR significantly increased the delivered capacities, more likely due to a better electrode structure. However, increasing the SBR amount to 4 wt.% decreased the reversible capacities, which can be explained by the poor swelling properties of SBR (i.e. non-polar material) in carbonate-based electrolytes [30,31]. In other words, in a high content SBR matrix, the K^+ diffusion resistance would become a limiting parameter. In addition, at high content, SBR could isolate the graphite particles from the electrolyte. Regarding the CE, the higher the SBR amount was, the lower the CE was, probably due to the formation of thicker

SEI with this SBR. At this point, a dedicated study will be necessary to confirm this phenomenon.

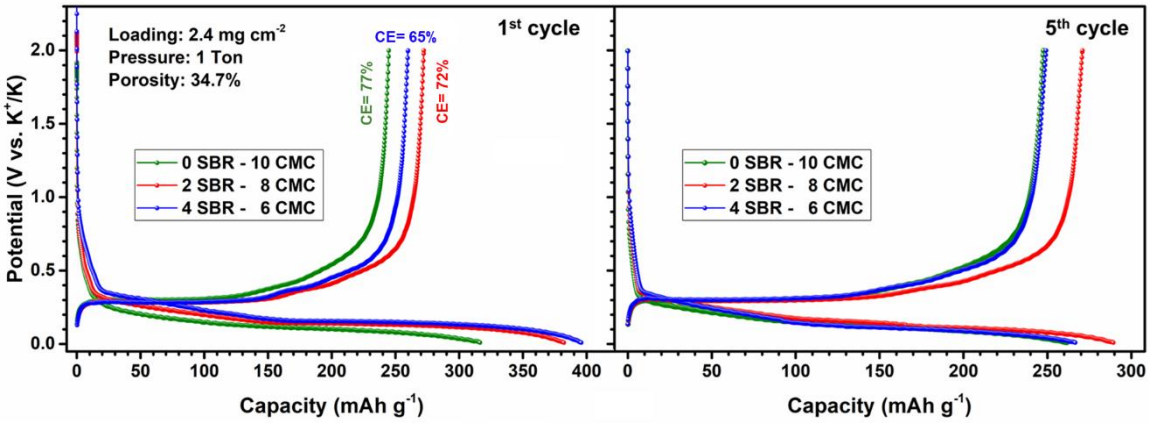

Figure 5. Galvanostatic profiles between 2-0.01V of the 1st and 5th cycle at C/20 for graphite electrodes (2.4 mg cm^{-2}, 5 wt.% CB and 35% porosity) as function of SBR/CMC amounts (0/10, 2/8 and 4/6 in wt.%).

To discriminate further the impact of carboxylated SBR, rate performance was then evaluated, **Figure 6a**. As expected, 2 wt.% SBR led to higher capacities from low (~270 mAh g^{-1} at C/20) to high rate (~165 mAh g^{-1} at C), which indicates an improvement of the electrode structure. This is confirmed by the lower polarization observed with 2 wt.% SBR during this rate test (**Figure S5**). At the opposite, 4 wt.% SBR led to worst rate performance (**Figure 6a**) and polarization (**Figure S5**). This confirms that at high content, SBR limits the K^+ diffusion in the electrolyte (due to its poor swelling properties in carbonates) and/or isolate graphite particles from the electrolyte. Galvanostatic intermittent titration technique (GITT) further confirmed that using 2 wt.% SBR led to a rather small polarization (0.15 V) compared to the other compositions (about 0.2 V) (**Figure S6**). Interestingly, such polarization is lower than the polarization observed for conventional carbonaceous electrodes in sodium and lithium ions batteries, as also reported elsewhere [3].

In addition, as K metal passivation upon cycling (i.e. K metal polarization increase) is more likely at the origin of the capacity decay observed during the conventional rate test (**Figure 6a**), an alternative test (see the experimental section) was performed to evaluate only the depotassiation rate capability (**Figure 6b**). For clarity, galvanostatic profiles are reported in **Figure S7**. Overall, much higher depotassiation capacities were obtained compared to the standard rate test. For instance, the best electrodes (with 2 wt.% SBR) delivered 243 mAh g^{-1}

during depotassiation at 5C using the alternative test (**Figure 6b**) compared to <20 mAh g^{-1} with the conventional test (**Figure 6a**). These results thus confirm that graphite can deliver high capacities at high depotassiation rate when the graphite potassiation is not limited by the K metal polarization. Finally, such alternative rate test is relevant when half-cells are used.

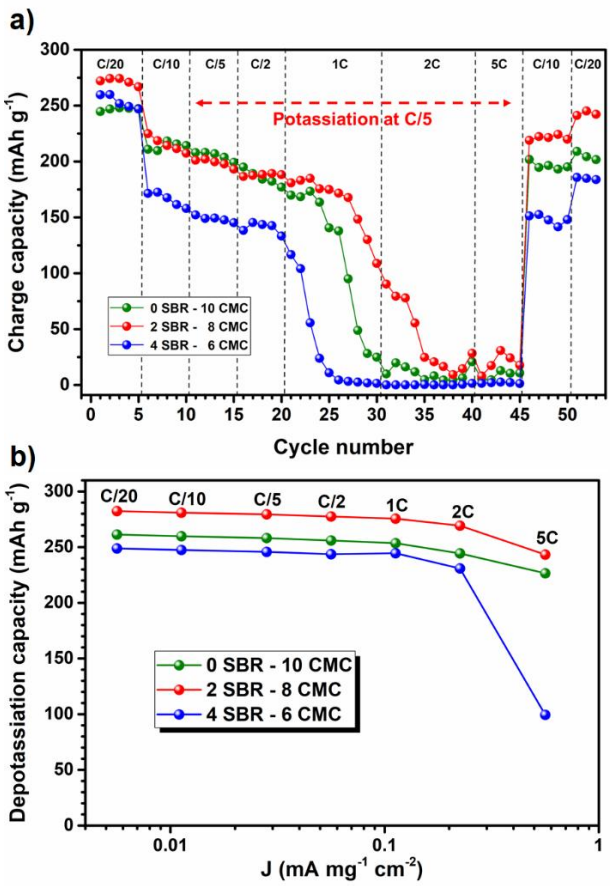

Figure 6. a) Galvanostatic rate performance between 2-0.01 V from C/20 to 5C and b) depotassiation capacities obtained using the alternative rate performance during the 5th cycle (successive depotassiation / 30 min relaxation steps) for graphite electrodes (2.4 mg cm^{-2}, 5 wt.% CB and 35% porosity) as function of SBR/CMC amounts (0/10, 2/8 and 4/6 in wt.%).

The effect of the SBR type (i.e. the functional groups content) was then evaluated, as reported in **Figure 7**. With the second SBR (SBR(2) from Synthomer), much higher CE were obtained during the formation cycles (**Figure 7c**), more likely due a better pre-formed SEI. Note that the exact effect of SBR (as CMC co-binder and depending of its type) on the SEI formation needs to be evaluated in a dedicated study in the future. Interestingly, during depotassiation at 5C, the polarization was significantly decreased using SBR(2) to 0.32 V compared to 0.78 V for the previous SBR (**Figure 7a**). As a result, during depotassiation at 5C, 94% of the

previous potassiation capacity (at C/20) was delivered using SBR(2) compared to only 81% with the previous SBR. Finally, with SBR(2), nearly no capacity loss was observed after 55 cycles compared to a 45% capacity loss with the previous SBR (**Figure 7c**). This is related to a lower volume expansion of the electrode with SBR(2), 11%, compared to 14% with SBR (**Table S3**). Interestingly, previous results without SBR (**Figure 4**) led to a much higher volume expansion (24%) after only 35 cycles (**Table S3**). Overall, these results thus highlight that appropriate carboxylated SBR significantly improves the electrode cohesion/elasticity (i.e. the volume expansion management) and thus the resulting power performance and capacity retention of graphite electrodes for KIBs. It is believed that the COO^- groups of the SBR binder may bond with the graphite/CB surfaces so that SBR(2) having an higher COO^- content, it will further increase the electrode cohesion/elasticity.

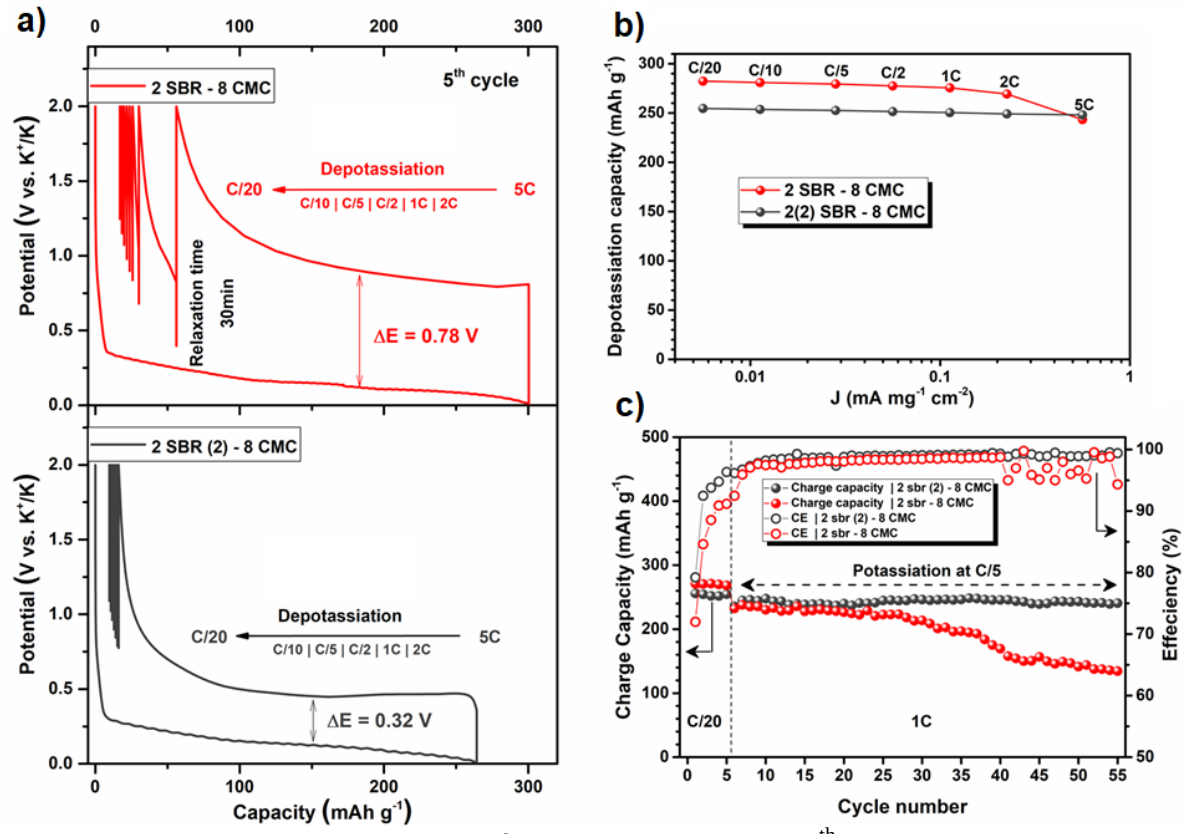

Figure 7. a) Galvanostatic rate performance during the 5th cycle between 2-0.01 V (successive depotassiation / 30 min relaxation steps) and b) corresponding depotassiation capacities for graphite electrodes (2.4 mg cm^{-2}, 5 wt.% CB, 8/2 wt.% CMC/SBR and 35% porosity). c) Capacity retention and coulombic efficiency obtained between 2-0.01 V at C/5 potassiation/1C depotassiation for graphite electrodes (2.4 mg cm^{-2}, 5 wt.% CB, 8/2 wt.% CMC/SBR and 35% porosity) with 2 SBR types.

Finally, the potassiation rate was also evaluated using a similar alternative rate test in 3-electrodes configuration (**Figure 8**). The use of SBR(2) led to 205 mAh g^{-1} during potassiation at 1C compared to only 55 mAh g^{-1} with CMC only. This result further highlights the interest of SBR(2) to significantly improve the potassiation rate capability of graphite electrode in KIBs. However, in this 3-electrodes configuration, the low K striping kinetics (**Figure S1**) may still limit the high rate graphite potassiation so that better performance could be obtained in full-cells.

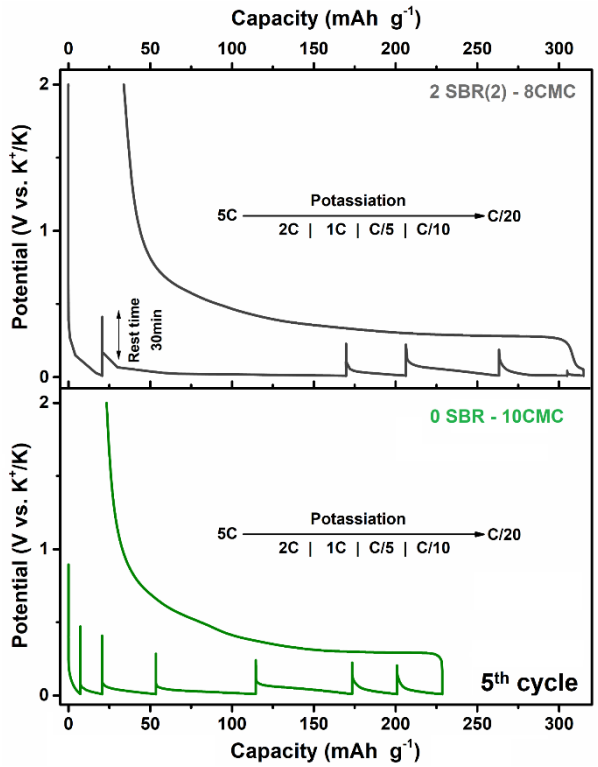

Figure 8. a) Alternative galvanostatic rate performance during the 5th cycle between 2-0.01 V using successive potassiation (from 5C to C/20) and 30 min relaxation steps for graphite electrodes (2.4 mg cm^{-2}, 5 wt.% CB and 35% porosity) using either 10 wt.% CMC or 8/2 wt.% CMC/SBR(2).

4. CONCLUSION

This work dealt with the optimization of the graphite electrodes formulation to enable high performance K-ion batteries. In a first step, optimal ionic (porosity) and electronic percolation networks were obtained by adjusting CB/graphite amounts as well as the electrode calendering pressure. Interestingly, 5 wt.% of CB led to better coulombic efficiency and power performance whatever the calendering pressure was, which points out the beneficial

role of optimizing the electronic network. In addition, the optimal balance between electronic and ionic properties was obtained for a 35% electrode porosity, while lowering the graphite loading from 4 to 2.4 mg cm^{-2} led to slight improvement. In second/third steps, optimal electrode structure/mechanical properties were then obtained by using carboxylated SBR with appropriate amount/functional groups contents as co-binder with the CMC. The best electrochemical performance were thus obtained by electrodes constituted of 95/5/8/2 wt.% of graphite(SLP30)/CB(C65)/CMC-Na/SBR(Synthomer) with 2.4 mg cm^{-2} loading and 35% porosity (pressed at 1 ton). Indeed, such graphite electrodes could delivered 92% (~250 mAh g^{-1}) of their capacity during depotassiation at 5C with a very low polarization (~0.3 V). These electrodes also delivered 205 mAh g^{-1} during potassiation at 1C (in 3-electrodes configuration) compared to only 55 mAh g^{-1} with CMC only. In addition, no capacity loss was observed after 50 cycles at C/5 potassiation/1C depotassiation due to a relatively low electrode volume expansion (11%) compared to 24% without SBR showed after 35 cycles at C/5 potassiation/1C depotassiation. Therefore, the use of carboxylated SBR (Synthomer) significantly improved the electrode structure/cohesion/elasticity, which led to much better rate performance, capacity retention as well as volume expansion management of graphite electrodes for KIBs. Finally, while further improvements could be obtained by tuning the electrolyte formulation (including the SEI formation), this work will benefit to the development of high energy KIBs.

ACKNOWLEDGEMENT

This work was part of the TROPIC project supported by Agence Nationale de la Recherche (ANR) under the grant ANR-19-CE05-0026.

REFERENCES

[1] D. Su, A. McDonagh, S. Qiao, G. Wang, High- Capacity Aqueous Potassium- Ion Batteries for Large- Scale Energy Storage, Adv. Mater. 29 (2017) 1604007. https://doi.org/10.1002/adma.201604007.

[2] T. Hosaka, K. Kubota, A.S. Hameed, S. Komaba, Research Development on K-Ion Batteries, Chem. Rev. 120 (2020) 6358–6466. https://doi.org/10.1021/acs.chemrev.9b00463.

[3] S. Komaba, T. Hasegawa, M. Dahbi, K. Kubota, Potassium intercalation into graphite to realize high-voltage/high-power potassium-ion batteries and potassium-ion capacitors, Electrochemistry Communications. 60 (2015) 172–175. https://doi.org/10.1016/j.elecom.2015.09.002.

[4] W. Zhang, Y. Liu, Z. Guo, Approaching high-performance potassium-ion batteries via advanced design strategies and engineering, Sci. Adv. 5 (2019) eaav7412. https://doi.org/10.1126/sciadv.aav7412.

[5] Z. Jian, W. Luo, X. Ji, Carbon Electrodes for K-Ion Batteries, J. Am. Chem. Soc. 137 (2015) 11566–11569. https://doi.org/10.1021/jacs.5b06809.

[6] J. Liu, T. Yin, B. Tian, B. Zhang, C. Qian, Z. Wang, L. Zhang, P. Liang, Z. Chen, J. Yan, X. Fan, J. Lin, X. Chen, Y. Huang, K.P. Loh, Z.X. Shen, Unraveling the Potassium Storage Mechanism in Graphite Foam, Adv. Energy Mater. 9 (2019) 1900579. https://doi.org/10.1002/aenm.201900579.

[7] T. Hosaka, S. Muratsubaki, K. Kubota, H. Onuma, S. Komaba, Potassium Metal as Reliable Reference Electrodes of Nonaqueous Potassium Cells, J. Phys. Chem. Lett. 10 (2019) 3296–3300. https://doi.org/10.1021/acs.jpclett.9b00711.

[8] J . Touja, V. Gabaudan, F. Farina, S. Cavaliere, L. Caracciolo, L. Madec, H. Martinez, A. Boulaoued, J. Wallenstein, P. Johansson, L. Stievano, L. Monconduit, Self-supported carbon nanofibers as negative electrodes for K-ion batteries: Performance and mechanism, Electrochimica Acta. 362 (2020) 137125. https://doi.org/10.1016/j.electacta.2020.137125.

[9] V. Gabaudan, L. Monconduit, L. Stievano, R. Berthelot, Snapshot on Negative Electrode Materials for Potassium-Ion Batteries, Front. Energy Res. 7 (2019) 46. https://doi.org/10.3389/fenrg.2019.00046.

[10] L. Wang, J. Yang, J. Li, T. Chen, S. Chen, Z. Wu, J. Qiu, B. Wang, P. Gao, X. Niu, H. Li, Graphite as a potassium ion battery anode in carbonate-based electrolyte and ether-based electrolyte, Journal of Power Sources. 409 (2019) 24–30. https://doi.org/10.1016/j.jpowsour.2018.10.092.

[11] T. Hosaka, T. Matsuyama, K. Kubota, S. Yasuno, S. Komaba, Development of KPF_6 /KFSA Binary-Salt Solutions for Long-Life and High-Voltage K-Ion Batteries, ACS Appl. Mater. Interfaces. 12 (2020) 34873–34881. https://doi.org/10.1021/acsami.0c08002.

[12] X. Niu, L. Li, J. Qiu, J. Yang, J. Huang, Z. Wu, J. Zou, C. Jiang, J. Gao, L. Wang, Salt-concentrated electrolytes for graphite anode in potassium ion battery, Solid State Ionics. 341 (2019) 115050. https://doi.org/10.1016/j.ssi.2019.115050.

[13] L. Fan, R. Ma, Q. Zhang, X. Jia, B. Lu, Graphite Anode for a Potassium-Ion Battery with Unprecedented Performance, Angewandte Chemie International Edition. 58 (2019) 10500–10505. https://doi.org/10.1002/anie.201904258.

[14 J. Zhang, Z. Cao, L. Zhou, G.-T. Park, L. Cavallo, L. Wang, H.N. Alshareef, Y.-K. Sun, J. Ming, Model-Based Design of Stable Electrolytes for Potassium Ion Batteries, ACS Energy Lett. 5 (2020) 3124–3131. https://doi.org/10.1021/acsenergylett.0c01634.

[15] Q. Li, Z. Cao, W. Wahyudi, G. Liu, G.-T. Park, L. Cavallo, T.D. Anthopoulos, L. Wang, Y.-K. Sun, H.N. Alshareef, J. Ming, Unraveling the New Role of an Ethylene Carbonate Solvation Shell in Rechargeable Metal Ion Batteries, ACS Energy Lett. 6 (2021) 69–78. https://doi.org/10.1021/acsenergylett.0c02140.

[16] L. Madec, V. Gabaudan, G. Gachot, L. Stievano, L. Monconduit, H. Martinez, Paving the Way for K-Ion Batteries: Role of Electrolyte Reactivity through the Example of Sb-Based Electrodes, ACS Appl. Mater. Interfaces. 10 (2018) 34116–34122. https://doi.org/10.1021/acsami.8b08902.

[17] L. Caracciolo, L. Madec, G. Gachot, H. Martinez, Impact of the Salt Anion on K Metal Reactivity in EC/DEC Studied Using GC and XPS Analysis, ACS Appl. Mater. Interfaces. 13 (2021) 57505–57513. https://doi.org/10.1021/acsami.1c19537.

[18] C. Meyer, H. Bockholt, W. Haselrieder, A. Kwade, Characterization of the calendering process for compaction of electrodes for lithium-ion batteries, Journal of Materials Processing Technology. 249 (2017) 172–178. https://doi.org/10.1016/j.jmatprotec.2017.05.031.

[19] R. Gonçalves, S. Lanceros-Méndez, C.M. Costa, Electrode fabrication process and its influence in lithium-ion battery performance: State of the art and future trends, Electrochemistry Communications. 135 (2022) 107210. https://doi.org/10.1016/j.elecom.2022.107210.

[20] Z. Xing, Y. Qi, Z. Jian, X. Ji, Polynanocrystalline Graphite: A New Carbon Anode with Superior Cycling Performance for K-Ion Batteries, ACS Appl. Mater. Interfaces. 9 (2017) 4343–4351. https://doi.org/10.1021/acsami.6b06767.

[21] Y. An, H. Fei, G. Zeng, L. Ci, B. Xi, S. Xiong, J. Feng, Commercial expanded graphite as a low–cost, long-cycling life anode for potassium–ion batteries with conventional carbonate electrolyte, Journal of Power Sources. 378 (2018) 66–72. https://doi.org/10.1016/j.jpowsour.2017.12.033.

[22] M. Carboni, A.J. Naylor, M. Valvo, R. Younesi, Unlocking high capacities of graphite anodes for potassium-ion batteries, RSC Adv. 9 (2019) 21070–21074. https://doi.org/10.1039/C9RA01931F.

[23] X. Wu, Z. Xing, Y. Hu, Y. Zhang, Y. Sun, Z. Ju, J. Liu, Q. Zhuang, Effects of functional binders on electrochemical performance of graphite anode in potassium-ion batteries, Ionics. 25 (2019) 2563–2574. https://doi.org/10.1007/s11581-018-2763-4.

[24] F. Jeschull, J. Maibach, Inactive materials matter: How binder amounts affect the cycle life of graphite electrodes in potassium-ion batteries, Electrochemistry Communications. 121 (2020) 106874. https://doi.org/10.1016/j.elecom.2020.106874.

[25] J. Park, N. Willenbacher, K.H. Ahn, How the interaction between styrene-butadiene-rubber (SBR) binder and a secondary fluid affects the rheology, microstructure and adhesive properties of capillary-suspension-type graphite slurries used for Li-ion battery anodes, Colloids and Surfaces A: Physicochemical and Engineering Aspects. 579 (2019) 123692. https://doi.org/10.1016/j.colsurfa.2019.123692.

[26] Y. Xiong, H. Xing, Y. Fan, Y. Wei, J. Shang, Y. Chen, J. Yan, SiO x -based graphite composite anode and efficient binders: practical applications in lithium-ion batteries, RSC Advances. 11 (2021) 7801–7807. https://doi.org/10.1039/D0RA10283K.

[27] T. Kwon, J.W. Choi, A. Coskun, The emerging era of supramolecular polymeric binders in silicon anodes, Chem. Soc. Rev. 47 (2018) 2145–2164. https://doi.org/10.1039/C7CS00858A.

[28] J.-H. Lee, S. Lee, U. Paik, Y.-M. Choi, Aqueous processing of natural graphite particulates for lithium-ion battery anodes and their electrochemical performance, Journal of Power Sources. 147 (2005) 249–255. https://doi.org/10.1016/j.jpowsour.2005.01.022.

[29] J.-Y. Eom, L. Cao, Effect of anode binders on low-temperature performance of automotive lithium-ion batteries, Journal of Power Sources. 441 (2019) 227178. https://doi.org/10.1016/j.jpowsour.2019.227178

[30] L. Wang, Y. Fu, V.S. Battaglia, G. Liu, SBR–PVDF based binder for the application of SLMP in graphite anodes, RSC Adv. 3 (2013) 15022. https://doi.org/10.1039/c3ra42773k.

[31] X. Li, J. Li, L. Ma, C. Yu, Z. Ji, L. Pan, W. Mai, Graphite Anode for Potassium Ion batteries: Current Status and Perspective, Energy Environ. Mater. (2021) eem2.12194. https://doi.org/10.1002/eem2.12194.

[32] N. Xiao, W.D. McCulloch, Y. Wu, Reversible Dendrite-Free Potassium Plating and Stripping Electrochemistry for Potassium Secondary Batteries, J. Am. Chem. Soc. 139 (2017) 9475–9478. https://doi.org/10.1021/jacs.7b04945.

[33] F. Allgayer, J. Maibach, F. Jeschull, Comparing the Solid Electrolyte Interphases on Graphite Electrodes in K and Li Half Cells, ACS Appl. Energy Mater. 5 (2022) 1136–1148. https://doi.org/10.1021/acsaem.1c03491.

[34] H. Buqa, M. Holzapfel, F. Krumeich, C. Veit, P. Novák, Study of styrene butadiene rubber and sodium methyl cellulose as binder for negative electrodes in lithium-ion batteries, Journal of Power Sources. 161 (2006) 617–622. https://doi.org/10.1016/j.jpowsour.2006.03.073.